

UC Davis

UC Davis Previously Published Works

Title

Foveal and Peripapillary Vascular Decrement in Migraine With Aura Demonstrated by Optical Coherence Tomography Angiography

Permalink

<https://escholarship.org/uc/item/90h5x1kx>

Journal

Investigative Ophthalmology & Visual Science, 58(12)

ISSN

0146-0404

Authors

Chang, Melinda Y
Phasukkijwatana, Nopasak
Garrity, Sean
[et al.](#)

Publication Date

2017-10-23

DOI

10.1167/iovs.17-22477

Copyright Information

This work is made available under the terms of a Creative Commons Attribution-NonCommercial-NoDerivatives License, available at <https://creativecommons.org/licenses/by-nc-nd/4.0/>

Peer reviewed

Foveal and Peripapillary Vascular Decrement in Migraine With Aura Demonstrated by Optical Coherence Tomography Angiography

Melinda Y. Chang,¹⁻³ Nopasak Phasukkijwatana,^{1,3,4} Sean Garrity,^{1,3} Stacy L. Pineles,^{1,3} Mansour Rahimi,^{1,3} David Sarraf,^{1,3} Mollie Johnston,⁵ Andrew Charles,⁵ and Anthony C. Arnold^{1,3}

¹Stein Eye Institute, University of California, Los Angeles, California, United States

²Doheny Eye Institute, University of California, Los Angeles, California, United States

³Department of Ophthalmology, University of California, Los Angeles, California, United States

⁴Department of Ophthalmology, Faculty of Medicine Siriraj Hospital, Mahidol University, Bangkok, Thailand

⁵Department of Neurology, University of California, Los Angeles, California, United States

Correspondence: Melinda Y. Chang, Department of Ophthalmology, the Stein Eye Institute, 100 Stein Plaza, University of California, Los Angeles, CA, USA; Melinda.y.wu@gmail.com.

Submitted: June 20, 2017

Accepted: September 28, 2017

Citation: Chang MY, Phasukkijwatana N, Garrity S, et al. Foveal and peripapillary vascular decrement in migraine with aura demonstrated by optical coherence tomography angiography. *Invest Ophthalmol Vis Sci.* 2017;58:5477-5484. DOI:10.1167/iov.17-22477

PURPOSE. Migraine, particularly with aura, has been associated with ocular and systemic ischemic complications, but there are limited data on the ocular vasculature in migraine. We used optical coherence tomography angiography (OCTA) to assess perfusion of the macula and optic nerve in migraine patients, with (MA) and without (MO) aura, compared to healthy controls (HC).

METHODS. We recruited 15 MA (mean age 42 years), 12 MO (mean age 46 years), and 22 HC (mean age 39 years) participants from neurology and neuro-ophthalmology clinics. Participants underwent optical coherence tomography and 3×3 mm OCTA of the macula and optic nerve. Foveal avascular zone area was automatically measured using AngioVue software, and vessel density was calculated as blood vessel length divided by scan area (mm^{-1}) after skeletonization of OCTA images.

RESULTS. On macular OCTA, MA participants had an enlarged foveal avascular zone area when compared with HC (0.300 ± 0.019 vs. 0.220 ± 0.066 mm^2 , $P = 0.006$). In addition, superficial foveal vessel density was decreased in MA participants when compared with MO participants (7.8 ± 0.31 vs. 9.3 ± 0.44 , $P = 0.04$) and HC (7.8 ± 0.31 vs. 9.4 ± 0.21 mm^{-1} , $P = 0.002$). On optic nerve OCTA, the MA participants had reduced superior peripapillary vessel density when compared with the MO participants (12.0 ± 0.45 vs. 14.0 ± 0.38 mm^{-1} , $P = 0.031$) and HC (12.0 ± 0.45 vs. 14.1 ± 0.53 mm^{-1} , $P = 0.035$). There were no significant differences between the MO and HC groups.

CONCLUSIONS. Migraine with, but not without, aura was associated with foveal and peripapillary vascular decrements, which may possibly mediate increased risk of ocular and systemic vascular complications in these patients. OCTA could potentially be useful as a biomarker for migraine with aura.

Keywords: migraine, OCT angiography, neuro-ophthalmology

Migraine is the third most common disease worldwide, with an overall prevalence of 14.7% (18.8% in females and 10.7% in males).¹ In one third of patients, migraine headaches are preceded by focal neurological disturbances, typically visual, which are termed “migraine auras.”² The pathophysiology of migraine is not fully elucidated, but a complex interplay of neural and vascular factors is likely involved.³ Migraine has been suggested as a risk factor for ischemic complications of the retina and optic nerve,⁴⁻⁹ in addition to systemic ischemic events including stroke and myocardial infarction.^{10,11} The associations are stronger for migraine with aura (MA) than migraine without aura (MO).^{10,12}

Ophthalmic disorders associated with migraine include branch and central retinal artery and vein occlusions⁴⁻⁷ as well as anterior and posterior ischemic optic neuropathy.^{8,9,13-16} In addition, migraine has been reported to be a risk factor for diagnosis and progression of normal tension glaucoma.^{17,18}

These disorders have been reported both during an acute attack of migraine^{4,7-9} as well as between attacks.^{5,15,17} Thus, there may be both acute and chronic changes of ocular perfusion in migraine patients that predispose migraineurs to the ocular complications previously described.

Despite this, there are limited data on the ocular vasculature in migraine patients. Rose et al.¹⁹ examined the retinal microvasculature in subjects with migraines using fundus photography and reported a higher incidence of retinopathy in migraine patients when compared with controls. Limitations of fundus photography include relatively low-resolution and poor visualization of deeper ocular vasculature including the deep capillary plexus and choroid. Recently, optical coherence tomography angiography (OCTA) has been developed and applied to imaging the microvasculature of both the macula and optic nerve.^{20,21} OCTA uses phase or amplitude decorrelation technology to image the



TABLE 1. Demographics and Clinical Data

Demographic and Clinical Measures	MA, n = 15	MO, n = 12	HC, n = 22
Mean age in years (range)	42 (18 to 64)	46 (29 to 58)	39 (18 to 66)
Male/female	5/10	3/9	14/8; * <i>P</i> = 0.03
Mean refractive error, SE (range)	-0.50 (-5.25 to +0.75)	-0.50 (-2.25 to +1.75)	-1.25 (-4.25 to plano)
Mean IOP, mm Hg (range)	16 (12 to 21)	13 (9 to 20)	16 (13 to 19)

MA, migraine with aura; MO, migraine without aura; HC, healthy controls; SE, spherical equivalent; IOP, intraocular pressure.

* *P* < 0.05, controls versus MO.

ophthalmic vasculature at a resolution of 5 μ m in three dimensions, allowing for segmentation with separate analysis of superficial and deep capillary networks.

We examined the macular and optic nerve vasculature in patients with migraine, with and without aura, using OCTA, and compared the findings with healthy controls. In addition, we evaluated the structural parameters of the macula and optic nerve using spectral-domain optical coherence tomography (OCT). Because of the potential risk of systemic and ocular ischemic events in migraine patients, especially those with aura, we hypothesized that the eyes of these patients would have an increased foveal avascular zone (FAZ) area when compared with controls. In addition, we hypothesized that migraine patients would have decreased vessel density (VD) in the macula and optic nerve as well as decreased foveal, ganglion cell complex (GCC), and retinal nerve fiber layer (RNFL) thickness.

METHODS

This study was approved by the University of California, Los Angeles Institutional Review Board and adhered to the tenets of the Declaration of Helsinki and Health Insurance Portability and Accountability Act. Informed consent was obtained from all participants after explanations of the nature and possible consequences of the study. We prospectively recruited patients diagnosed with migraine, with and without aura, from neurology and ophthalmology clinics. Healthy controls (HC) were recruited from ophthalmology clinics and among faculty and staff members at the University of California, Los Angeles. All participants were 18 years of age or older. Participants with migraine met the International Classification of Headache Disorders 3 criteria for diagnosis of migraine with aura (MA) or migraine without aura (MO),²² and most were under the care of a neurologist specializing in headache disorders (MJ, AC). HC reported either no headaches or headaches not meeting the International Classification of Headache Disorders 3 criteria for migraines.²² In particular, healthy controls who experienced any headaches were required to have the absence of all of the following International Classification of Headache Disorders 3 characteristics of migraines: moderate or severe pain intensity, aggravation by or causing avoidance of routine physical activity, nausea, vomiting, photophobia, and phonophobia. Exclusion criteria for all groups included any neurologic disorder other than migraine (including neurodegenerative diseases such as Alzheimer's or Parkinson's diseases); any disorder of the optic nerve (including glaucoma) or retina; history of intraocular surgery other than cataract extraction, refractive error greater than +3.00 or less than -6.00 diopters; systemic conditions affecting microvasculature such as diabetes mellitus, hypertension, vasculitis, or renal disease; and ocular media opacity precluding high-quality imaging. Healthy controls were also excluded if taking vasoactive medications such as calcium channel blockers. Demographic

data for 15 MA, 12 MO, and 22 HC participants who met inclusion and exclusion criteria are shown in Table 1.

Ophthalmologic Examination

All participants underwent full ophthalmologic examination of each eye by a neuro-ophthalmologist (MYC, ACA) or retina specialist (DS), including best-corrected visual acuity, refractive error based on manifest refraction (if visual acuity was worse than 20/20), or habitual glasses prescription, IOP (measured by iCare tonometer [Finland Oy, Vantaa, Finland] or Goldmann applanation [Haag-Streit, Koniz, Switzerland], depending on instrument availability), pupil size and reactivity, color vision testing by Ishihara plates, visual fields by confrontation, extraocular motility and alignment, slit lamp examination, and fundus examination of the posterior pole.

Acquisition of Images

All participants underwent OCT and OCTA imaging using the RTVue XR Avanti spectral-domain OCT device with AngioVue software (Optovue, Inc., Fremont, CA, USA). This instrument uses a light source at 840 nm with a bandwidth of 45 nm and A-scan rate of 70,000 scans per second. OCT and OCTA images were excluded if the signal strength index was less than 45 or if the automated algorithm failed to correctly segment the image.

OCT Angiography Scans. OCTA images of the macula and optic nerve were both acquired in a 3 \times 3 mm cube, each containing 304 \times 304 scans. Two scans, one horizontal and one vertical, were obtained and merged to minimize motion artifact. Split-spectrum amplitude decorrelation technology was used to improve the signal-to-noise ratio.

Structural OCT Scans. The macula was imaged using the macula line protocol, consisting of a 9.0-mm b-scan centered on the fovea generated by averaging 65 frames. A 6.0 \times 6.0 mm volume scan of the optic nerve was generated using the three-dimensional (3D) disc protocol, which was used as a baseline for RNFL. The peripapillary RNFL was imaged using the optic nerve head (ONH) protocol, which evaluated RNFL thickness along a 3.45-mm diameter circle centered on the optic nerve head. The GCC, which includes the RNFL, ganglion cell layer, and inner plexiform layer, was imaged in a 6.0 \times 6.0 mm circular area in the macula using the GCC scan protocol.

Analysis of Images

OCT Angiography Scans. Each scan was automatically segmented by the AngioVue software (Fig. 1). In the case of macular scans, the superficial retinal capillary plexus (SCP) was segmented with an inner boundary 3 μ m posterior to the internal limiting membrane (ILM) and outer boundary 15 μ m posterior to the outer aspect of the inner plexiform layer (IPL; Fig. 1A). The deep retinal capillary plexus (DCP) was segmented with an inner boundary 15 μ m posterior to the outer aspect of the IPL and outer boundary 70 μ m posterior to the outer aspect of the IPL (Fig. 1B). Optic nerve scans were segmented into ONH and radial peripapillary capillary (RPC)

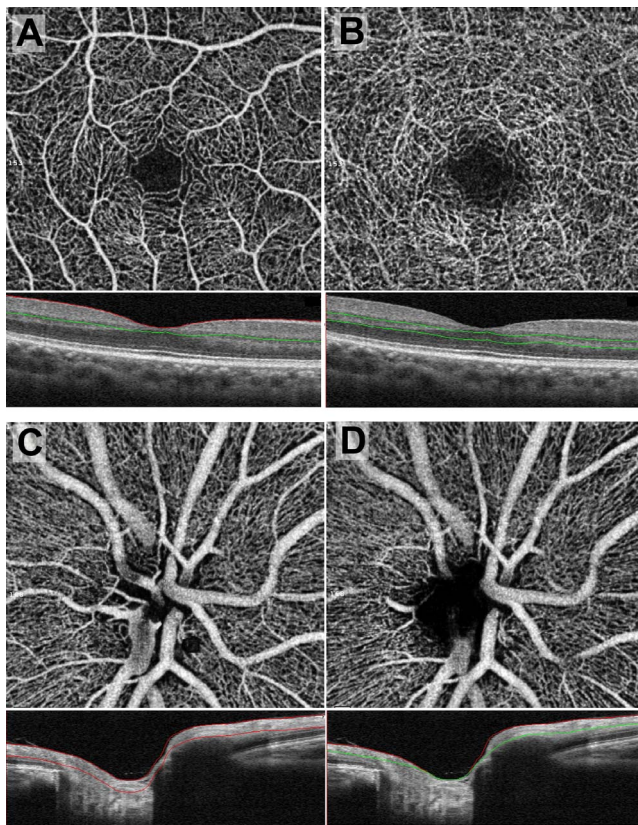


FIGURE 1. En face OCTA scans with the corresponding b-scan OCT shown immediately *below*. The level of segmentation is between the *red* and/or *green* lines on the OCT. (A) Superficial retinal capillary plexus, (B) deep retinal capillary plexus, (C) ONH slab, (D) RPC slab.

slabs. The ONH slab was segmented with an inner boundary at the anterior border of the ILM and an outer boundary 150 μ m posterior to the ILM (Fig. 1C). The RPC slab was delimited with an inner boundary at the ILM and an outer boundary at the posterior aspect of the RNFL (Fig. 1D). The ONH slab was used to measure whole-image and ONH VD, whereas the RPC slab was used to measure peripapillary VD.

The following measures were extracted from en face OCTA images of the macula: FAZ area and VD in the SCP and DCP. The FAZ area was measured using AngioVue software using a slab from the internal limiting membrane (ILM) to 75 μ m above the retinal pigment epithelium. Although prior OCTA studies reported the FAZ area separately for the SCP and DCP, more recent histologic and OCTA data suggest that a

single merged quantitative measurement is more accurate because of the convergence of the SCP and DCP in the parafoveal region.²³ Quantitative analysis of VD in the SCP and DCP was performed as previously described by Iafe and colleagues.²⁰ Briefly, the OCTA en face images were exported and raw images were imported into ImageJ²⁴ (provided in the public domain by the U.S. National Institutes of Health, Rockville, MD, USA). The images were then made binary and skeletonized, converting each blood vessel to a one-pixel wide line. The number of black pixels representing blood vessels was extracted using histogram analysis. Vessel density was calculated as: [(pixels of blood vessels) \times (scan width in mm/pixels per scan width)]/area in mm^2 , resulting in a density with a unit of mm^{-1} . The VD was calculated in the whole 3×3 mm image (Fig. 2A,B) as well as a 1×1 mm circle centered on the fovea (Fig. 2C).

En face OCTA images of the optic nerve in the ONH and RPC segments were similarly exported and analyzed using ImageJ (Fig. 3). The whole-image VD was assessed using the ONH segment (Fig. 3B). A scanning laser ophthalmoscope image acquired at the time of OCTA was superimposed on the skeletonized OCTA image to outline the borders of the ONH (Fig. 3C). VD within the borders of the ONH was then calculated (Fig. 3D). The RPC image was processed in the same manner (Figs. 3E–H). Peripapillary VD was assessed in a ring measuring 0.5 mm in width encircling the optic nerve head on the RPC segment of the OCTA. The peripapillary ring was divided into superior and inferior halves, and the VD was separately analyzed in these two hemispheres.

In addition to angiography images, the Optovue software automatically measures retinal thickness from the macular OCTA scans. The foveal thickness of each eye, measured at the center of the fovea and spanning the entire retina, from the ILM to retinal pigment epithelium was recorded.

Structural OCT Scans. Structural OCT scans of the macula and optic nerve were reviewed by an ophthalmologist (MYC) to exclude the possibility of retinal or optic nerve pathology, including glaucoma. Any macular pathology, such as drusen or epiretinal membrane, resulted in exclusion of the affected eye from the study. Glaucoma was defined as IOP greater than 21 mm Hg with characteristic glaucomatous optic nerve cupping on examination and/or RNFL thinning on OCT. Eyes with any optic nerve pathology including glaucoma were excluded.

The following measurements were recorded from the OCT RNFL scans for each eye: average RNFL thickness and thickness in each quadrant (superior, temporal, inferior, and nasal). The average, superior, and inferior GCC thickness measurements were also recorded.

Power Calculation. Based on the first five participants in each group who underwent OCTA scans, a power calculation

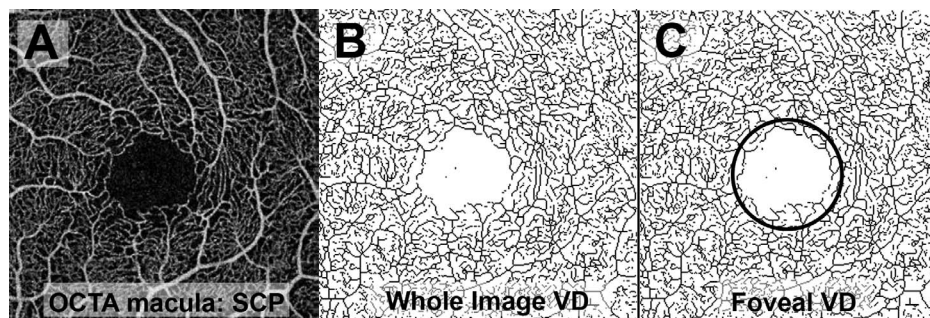


FIGURE 2. Processing of macular OCTA scans for measurement of VD. (A) Raw image of macular OCTA scan of the SCP. (B) The raw image was made binary and skeletonized for calculation of whole image vessel density. (C) A 1×1 mm circular area centered on the fovea was selected for measurement of foveal VD.

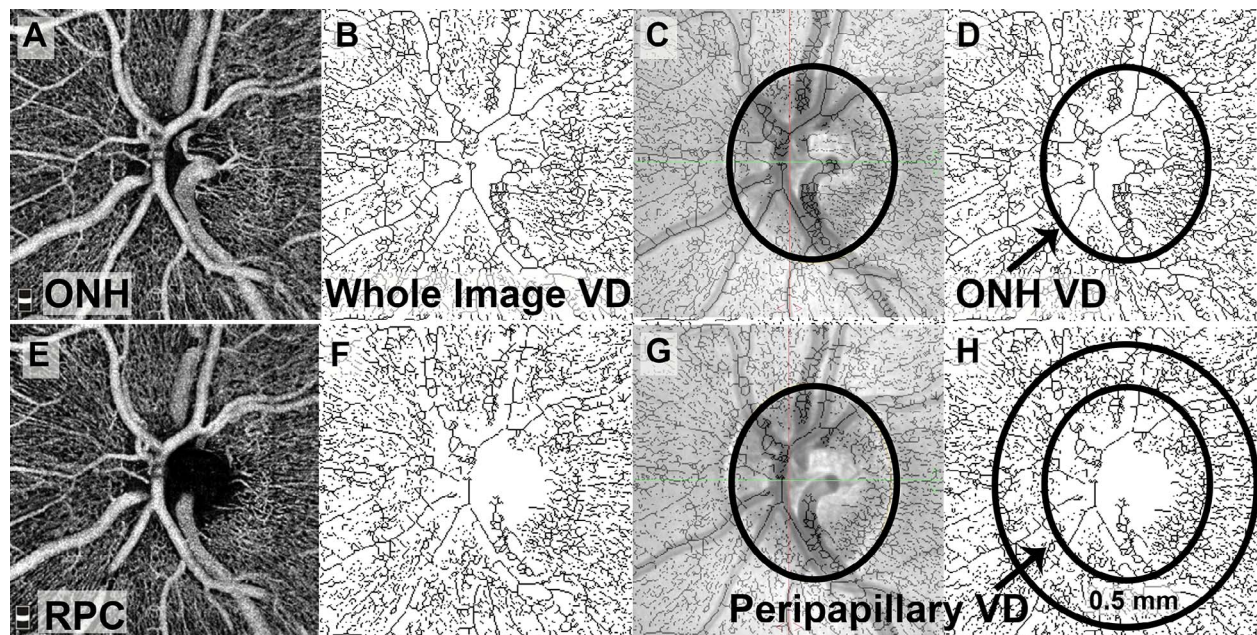


FIGURE 3. Processing of optic nerve OCTA scans for measurement of whole-image VD, ONH VD, and peripapillary VD. The ONH segment (A) was used for assessment of the whole image and ONH VD. After the raw image was made binary and skeletonized (B), the scanning laser ophthalmoscopy (SLO) image was superimposed on the skeletonized image to trace the borders of the ONH (C). The area within the ONH borders was used to assess ONH VD (D). The RPC segment was used to assess peripapillary VD (E). The raw image was similarly made binary and skeletonized (F), and the SLO image was used to trace the borders of the ONH (G). A ring 0.5 mm in width around the ONH was selected, and the peripapillary VD was assessed within this ring (H).

was performed to determine the number of participants required to detect a significant difference in foveal avascular zone area, the primary outcome in this study. We found that 14 participants would be required in each group to detect a difference of 0.1 mm^2 with a type I error (α) of 0.05 and a type II error (β) of 0.20.

Statistical Analysis

OCT and OCTA measurements of the optic nerve and retina were compared between MA, MO, and control participants using 2-way repeated measures analysis of variance to account for inclusion of both eyes per participant. Subgroup analysis was performed by gender; female participants were compared with female controls, and male participants were compared with male controls. *P* values less than 0.05 were considered significant.

RESULTS

We recruited 15 MA, 12 MO, and 22 healthy control participants. The mean ages for the MA, MO, and HC participants were 42, 46, and 39 years, respectively, and did not significantly differ among groups ($P > 0.08$; Table 1). There were significantly more males in the control group when compared with the MO group ($P = 0.03$). The mean refractive error and intraocular pressure were not significantly different among the groups ($P > 0.05$). All macular OCTA images except one were of sufficient quality for study inclusion. Five optic nerve OCTA images were excluded because of poor quality (signal strength index less than 45), and two optic nerve OCTA scans were excluded as a result of the failure of the automated segmentation algorithm.

Representative OCTA scans of the MA, MO, and HC participants are shown in Figures 4 (macula) and 5 (optic nerve). Quantitative analysis of macular OCTA findings in the

MA, MO, and HC participants is shown in Table 2. The FAZ area measured $0.300 \pm 0.019 \text{ mm}^2$ in the MA participants, significantly larger than the control participants ($0.220 \pm 0.066 \text{ mm}^2$, $P = 0.006$). In addition, the foveal VD in the SCP was significantly lower in the MA participants ($7.8 \pm 0.31 \text{ mm}^{-1}$) when compared with both the MO (9.3 ± 0.44 , $P = 0.04$) and control (9.4 ± 0.21 , $P = 0.002$) participants. There were no significant differences between the MO and control participants. In addition, there was no significant difference among the MA, MO, and control participants in whole-image VD in the macula in the SCP or any measure in the DCP ($P > 0.09$).

The optic nerve OCTA measurements in the MA, MO, and HC participants are displayed in Table 3. The superior peripapillary VD was significantly reduced in the MA participants ($12.0 \pm 0.45 \text{ mm}^{-1}$) when compared with both the MO ($14.0 \pm 0.38 \text{ mm}^{-1}$, $P = 0.031$) and control ($14.1 \pm 0.53 \text{ mm}^{-1}$, $P = 0.035$) participants. However, there was no significant difference among the groups in whole-image VD, optic nerve VD, total peripapillary VD, and inferior peripapillary VD ($P > 0.09$).

The structural OCT measurements including the foveal, RNFL, and GCC thickness in the MA, MO, and HC participants are shown in Table 4. The MA participants demonstrated borderline thinner average RNFL ($97 \pm 1.8 \mu\text{m}$) when compared with the HC participants ($104 \pm 2.1 \mu\text{m}$, $P = 0.05$). In addition, the superior RNFL was marginally thinner in the MA participants ($116 \pm 2.4 \mu\text{m}$) when compared with the HC participants (127 ± 3.9 , $P = 0.049$). There was no significant difference among the groups in the thickness of other quadrants of the RNFL ($P > 0.08$). In addition, there was no significant difference among the groups in foveal ($P > 0.43$) or GCC ($P > 0.22$) thickness.

Subgroup analysis by gender showed that female MA participants had an enlarged FAZ area when compared with the female MO participants (0.346 vs. 0.224 mm^2 , $P = 0.017$)

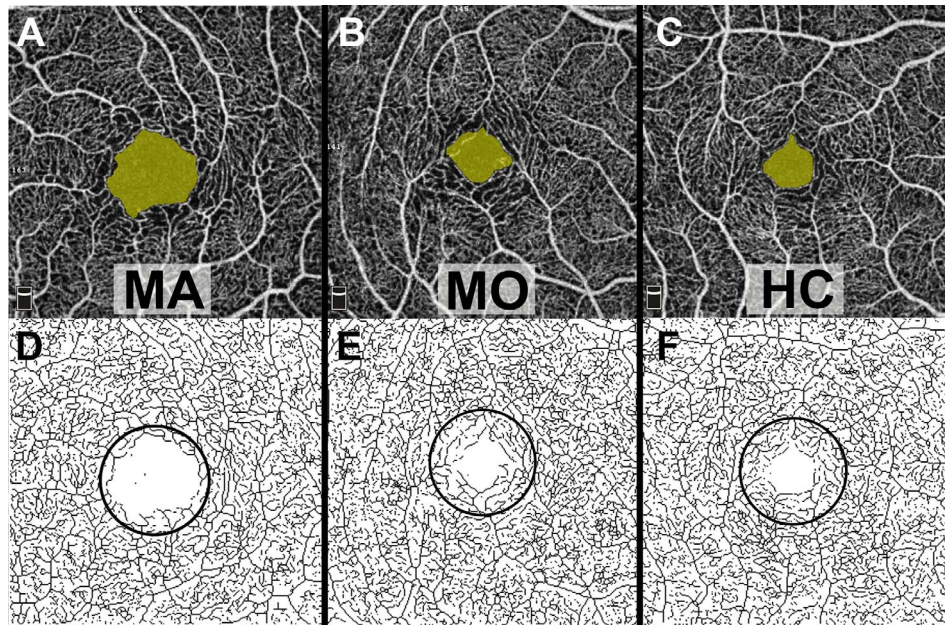


FIGURE 4. Representative macular OCTA scans of MA, MO, and HC participants. The FAZ area is shaded yellow in the top row. In the bottom row, the skeletonized OCTA images of the SCP were used for the assessment of foveal VD within the outlined 1 × 1 mm circular area. Qualitatively, the FAZ area is enlarged and foveal VD decreased in the MA participant when compared with the MO and HC participants.

and female HC participants (0.346 vs. 0.204 mm², $P = 0.012$). In addition, the female MA participants had decreased superficial foveal VD when compared with the female HC participants (7.3 vs. 10.4 mm⁻¹, $P = 0.002$). There were no significant differences on macular OCTA between the female MO patients and the female HC participants ($P > 0.33$). There were also no significant differences in macular OCTA measures among male participants in the MA, MO, and HC groups ($P > 0.07$). Decreased superior peripapillary VD by OCTA of the

optic nerve was found in both the female and male MA participants ($P < 0.04$).

DISCUSSION

We demonstrated by OCTA that MA, but not MO, patients had a significantly enlarged FAZ area and reduced superficial foveal VD when compared with the HC participants. In addition,

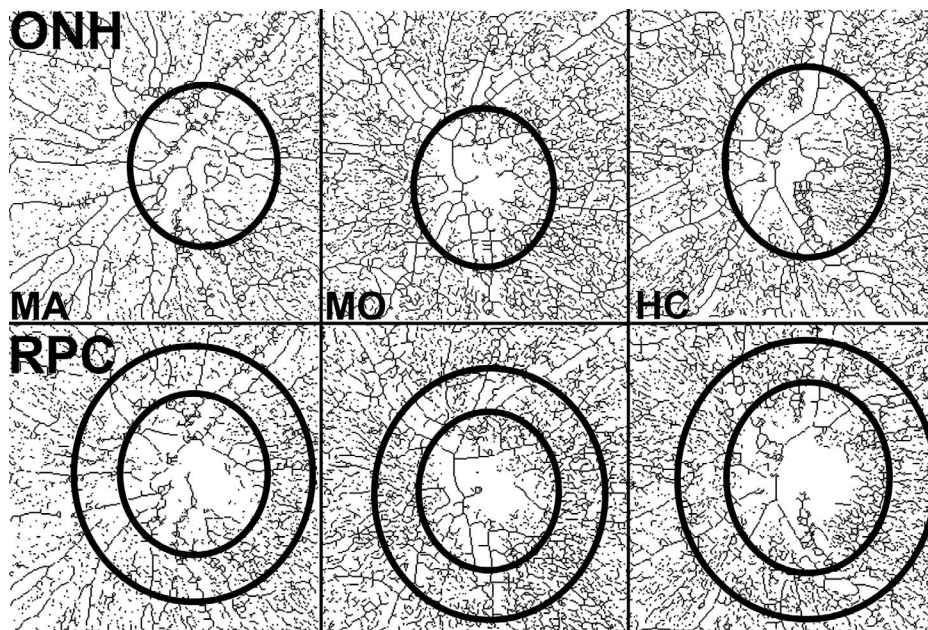


FIGURE 5. Representative skeletonized OCTA scans of the optic nerve, segmented on the ONH in the top row and the RPC in the bottom row, in eyes of MA, MO, and HC participants. The ellipses in the top row outline the borders of the ONH. In the bottom row, the inner ellipse demarcates the ONH border, and the larger ellipse shows the outer border of the ring used to assess peripapillary VD. Qualitatively, the peripapillary VD is lower in the MA participant when compared with the MO and HC participants.

TABLE 2. Macular OCTA Measurements in MA, MO, and HC Participants

Macular OCTA Measures	MA	MO	HC
Foveal avascular zone size, mm ²	0.300 ± 0.019	0.232 ± 0.019	0.220 ± 0.066, †P = 0.006
SCP			
Whole-image macular VD, mm ⁻¹	15.3 ± 0.47	15.9 ± 0.39	15.8 ± 0.32
Foveal VD, mm ⁻¹	7.8 ± 0.31	9.3 ± 0.44, *P = 0.04	9.4 ± 0.21, †P = 0.002
DCP			
Whole-image macular VD, mm ⁻¹	19.2 ± 0.29	19.4 ± 0.36	19.6 ± 0.23
Foveal VD, mm ⁻¹	7.9 ± 0.34	8.8 ± 0.54	8.1 ± 0.30

All values indicate mean ± standard error of mean. Bold values indicate significance between groups ($P < 0.05$). SCP, superficial retinal capillary plexus; DCP, deep retinal capillary plexus; VD, vessel density.

* $P < 0.05$, MA versus MO.

† $P < 0.05$, MA versus HC.

optic nerve OCTA showed that MA, but not MO, participants had significantly decreased superior peripapillary VD.

The increased FAZ area found in the MA participants suggests the possibility of a microangiopathy affecting the retina. This is important in light of possible systemic vascular risks of migraine with aura, including stroke and cardiovascular disease.^{10,11} The enlargement of the FAZ area may be a result of microvascular ischemic events or capillary remodeling adjacent to the normal FAZ, as has been suggested in other systemic disorders such as diabetes^{25,26} and sickle cell disease.^{27,28} Because this is a cross-sectional study, it is unclear whether the FAZ changes are the result of ischemia in the context of acute migrainous attacks or a systemic vasculopathy that predisposes to both retinal microvascular alterations and migraine with aura.

The finding of decreased foveal vessel density in the SCP in the MA participants is also supportive of retinal microvascular disease. Although we did not find a significant difference in the DCP, there was a trend toward lower foveal VD in the MA group. Assessment of VD in the DCP is hindered by projection artifact, which is caused by the shadow of superficial blood vessels projecting onto deeper layers.²³ This artifact may have contributed to the inability to detect a significant difference in the DCP; alternatively, the sample size may have been insufficient, as the power calculation was based on the difference in FAZ area rather than VD among the groups.

The chronic retinovascular alterations demonstrated by OCTA in the MA participants may be related to the increased risk of ocular complications in migraine patients, even in the absence of an acute attack. Greven et al.⁵ reported that 25% of young adults with retinal arterial occlusions had a history of migraines, and none were acutely symptomatic at the time of the event. Furthermore, a history of migraine has been reported in association with paracentral acute middle maculopathy, an ischemic disorder of the middle and deep capillary plexus in the macula.²⁹

The finding of decreased peripapillary VD superiorly in the MA patients has potential implications for optic nerve

disorders such as ischemic optic neuropathy and normal-tension glaucoma. Both anterior and posterior ischemic optic neuropathy have been reported in association with migraines,^{8,9,13,14,30} and Arnold et al.¹⁵ found that a history of migraine was a risk factor for non-arteritic anterior ischemic optic neuropathy in patients younger than 50 years.

Migraine has also been associated with normal tension glaucoma.^{17,18} Among patients enrolled in the multicenter randomized clinical trial, the Collaborative Normal Tension Glaucoma Study, migraine was associated with an increased risk of progression without treatment.¹⁷ The relative risk for progression in migraine patients was 2.58, similar to that of patients with disc hemorrhages (2.72). Our findings suggest that the relationship between migraine and normal tension glaucoma may be mediated by chronic reduction in peripapillary perfusion in the MA participants. OCTA studies in normal tension glaucoma patients demonstrate decreased peripapillary perfusion, and the amount of reduction correlates with several measures of disease severity.³¹

By structural OCT, we found borderline decreased average and superior RNFL thickness in MA, but not MO, participants when compared with controls. This corresponds to the superior peripapillary VD decrement demonstrated in MA participants by OCTA. There were no differences in foveal or GCC thickness. Given the relatively small absolute difference in RNFL thickness between the groups (7 to 11 μm) and the marginally significant P values (0.049 and 0.05), larger studies are required to assess whether the RNFL is truly thinned in the MA patients. Prior structural OCT studies in migraine patients have shown conflicting results.³²⁻³⁸

By subgroup analysis, we found that the macular OCTA differences in the MA participants were significant only in females. This is consistent with the report that females with migraine with aura have a higher risk of systemic ischemic complications such as stroke.³⁹ The pathophysiology of the relationship between gender and ischemia in migraine is not fully understood, but may be related to the effect of estrogen and progesterone on endothelial cells.⁴⁰

TABLE 3. OCTA Measurements in MA, MO, and HC Participants

Optic Nerve OCTA Measures	MA	MO	HC
Whole-image VD, mm ⁻¹	12.5 ± 0.34	13.8 ± 0.26	13.3 ± 0.30
ONH VD, mm ⁻¹	9.8 ± 0.22	10.5 ± 0.28	9.9 ± 0.31
Peripapillary VD, mm ⁻¹	12.2 ± 0.41	13.6 ± 0.34	13.4 ± 0.33
Superior peripapillary VD, mm ⁻¹	12.0 ± 0.45	14.0 ± 0.38, *P = 0.031	14.1 ± 0.53, †P = 0.035
Inferior peripapillary VD, mm ⁻¹	12.5 ± 0.51	13.2 ± 0.46	12.6 ± 0.29

All values indicate mean ± standard error of mean of VD in the area indicated. Bold values indicate significance between groups ($P < 0.05$). ONH, optic nerve head.

* $P < 0.05$, MA versus MO.

† $P < 0.05$, MA versus HC.

TABLE 4. Thickness Measurements of the Macula, Retinal Nerve Fiber Layer, and Ganglion Cell Complex in MA, MO, and HC Participants by OCT

Structural OCT Measures	MA	MO	HC
Macula			
Fovea, μm	255 \pm 4.2	262 \pm 4.0	260 \pm 2.4
Retinal nerve fiber layer			
Average, μm	97 \pm 1.8	99 \pm 1.9	104 \pm 2.1, †P = 0.050
Superior, μm	116 \pm 2.4	121 \pm 3.2	127 \pm 3.9, †P = 0.049
Inferior, μm	122 \pm 3.1	122 \pm 2.9	131 \pm 2.6
Temporal, μm	76 \pm 1.5	73 \pm 1.4	80 \pm 2.4
Nasal, μm	74 \pm 2.7	79 \pm 2.0	80 \pm 2.2
Ganglion cell complex			
Average, μm	96 \pm 1.0	96 \pm 1.2	98 \pm 1.7
Superior, μm	96 \pm 1.0	95 \pm 1.1	97 \pm 1.8
Inferior, μm	96 \pm 1.0	97 \pm 1.3	99 \pm 1.7

All values indicate mean \pm standard error of mean. Bold values indicate significance between groups ($P < 0.05$).

† $P < 0.05$, MA versus HC.

Our study has several limitations. The sample size was relatively small—power analysis led us to the goal of recruiting 14 participants per group, and we successfully recruited more than 14 MA and control participants, but only 12 MO participants. Because this study was powered to assess the primary outcome, the difference in FAZ area between the groups, the study was underpowered to detect smaller differences in other measures, especially when multiple comparisons are considered. Future studies specifically designed to assess measures other than FAZ area, such as optic nerve OCTA and OCT changes in migraine, will require a larger sample size.

We did not find significant differences in the DCP on macular OCTA scans, and this may have been in part because of the projection artifact, which introduces error in assessment of the DCP. Recently, new software for projection artifact removal has been developed that should improve the accuracy of DCP measurements. However, we did not utilize this software as it was not available at the time of image analysis for this study. In addition, one macular OCTA and seven optic nerve OCTA scans were excluded because of poor quality. This represents only 7% of the total number of OCTA scans performed, so we believe these missing scans were unlikely to bias our results but cannot exclude this possibility. The greater number of poor quality optic nerve OCTA scans may be a result of the difficulty with eccentric fixation required to image the optic nerve, or participant fatigue, as optic nerve scans were always performed after macular scans in our study protocol. Furthermore, although we excluded scans with obvious segmentation failures (such as segmentation within the vitreous cavity), we did not manually correct for subtle errors of automatic segmentation as may occur, for example, in eccentric scans with increased reflectivity of Henle's fiber layer.⁴¹ Finally, although our study protocol excluded normal participants on medications with vasoactive effects, we did not control for medications used by the MA and MO participants. However, an equal percentage of patients in both groups (7 of 15 MA, and 6 of 12 MO) were taking triptans, which is a class of migraine medications that has been associated with vasoconstriction.³⁹ This reduces but does not eliminate the chance of medications confounding our comparison of MA and MO participants.

In conclusion, we report enlarged FAZ area and decreased VD in the superficial fovea and superior peripapillary region in the eyes of MA, but not MO, participants when compared with

healthy controls. These findings may mediate the increased risk of ocular complications such as retinovascular occlusion, ischemic optic neuropathy, and normal tension glaucoma in some patients with migraines. In addition, ocular perfusion abnormalities may reflect vasculopathy in the cerebral or systemic circulations. Further studies are necessary to determine whether OCTA findings in MA participants correlate with a possible increased risk of ocular and systemic vascular events. If such an association is found, OCTA could potentially be useful as a fast, noninvasive, and relatively inexpensive biomarker in patients with migraine with aura.

Acknowledgments

Presented at North American Neuro-Ophthalmology Society Annual Meeting, Washington, D.C., United States, 2017; Association for Research in Vision and Ophthalmology Annual Meeting, Baltimore, Maryland, United States, 2017; and accepted for presentation at the Women in Ophthalmology 2017 Summer Symposium, San Diego, California, United States, 2017.

Supported by National Institutes of Health/National Eye Institute (NIH/NEI, Bethesda, MD, USA) Grant K23EY021762, Research to Prevent Blindness, Walt and Lily Disney Award for Amblyopia Research, Knights Templar Eye Foundation (Flower Mound, TX, USA) Oppenheimer Family Foundation (Chicago, IL, USA).

Disclosure: **M.Y. Chang**, None; **N. Phasukkijwatana**, None; **S. Garrity**, None; **S.L. Pineles**, None; **M. Rahimi**, None; **D. Sarraf**, Allergan (F), Genentech (C, F), Regeneron (F), Optovue (C, F); **M. Johnston**, None; **A. Charles**, None; **A.C. Arnold**, None

References

- Vos T, Flaxman AD, Naghavi M, et al. Years lived with disability (YLDs) for 1160 sequelae of 289 diseases and injuries 1990-2010: a systematic analysis for the Global Burden of Disease Study 2010. *Lancet*. 2012;380:2163-2196.
- Rasmussen BK, Olesen J. Migraine with aura and migraine without aura: an epidemiological study. *Cephalalgia*. 1992; 12:221-228; discussion 186.
- Jacobs B, Dussor G. Neurovascular contributions to migraine: moving beyond vasodilation. *Neuroscience*. 2016;338:130-144.
- Berversdorf D, Stommel E, Allen C, Stevens R, Lessell S. Recurrent branch retinal infarcts in association with migraine. *Headache*. 1997;37:396-399.
- Greven CM, Slusher MM, Weaver RG. Retinal arterial occlusions in young adults. *Am J Ophthalmol*. 1995;120: 776-783.
- Graveson GS. Retinal arterial occlusion in migraine. *Br Med J*. 1949;2:838-840.
- Coppeto JR, Lessell S, Sciarra R, Bear L. Vascular retinopathy in migraine. *Neurology*. 1986;36:267-270.
- Katz B. Bilateral sequential migrainous ischemic optic neuropathy. *Am J Ophthalmol*. 1985;99:489.
- Lee AG, Brazis PW, Miller NR. Posterior ischemic optic neuropathy associated with migraine. *Headache*. 1996;36: 506-510.
- Kruit MC, van Buchem MA, Hofman PA, et al. Migraine as a risk factor for subclinical brain lesions. *JAMA*. 2004;291:427-434.
- Sacco S, Kurth T. Migraine and the risk for stroke and cardiovascular disease. *Curr Cardiol Rep*. 2014;16:524.
- Kurth T, Schurks M, Logroscino G, Gaziano JM, Buring JE. Migraine, vascular risk, and cardiovascular events in women: prospective cohort study. *BMJ*. 2008;337:a636.
- Weinstein JM, Feman SS. Ischemic optic neuropathy in migraine. *Arch Ophthalmol*. 1982;100:1097-1100.

14. Foroozan R, Marx DP, Evans RW. Posterior ischemic optic neuropathy associated with migraine. *Headache*. 2008;48:1135-1139.
15. Arnold AC, Costa RM, Dumitrascu OM. The spectrum of optic disc ischemia in patients younger than 50 years (an American Ophthalmological Society thesis). *Trans Am Ophthalmol Soc*. 2013;111:93-118.
16. Arnold AC. The 14th Hoyt lecture: ischemic optic neuropathy: the evolving profile, 1966-2015. *J Neuroophthalmol*. 2016;36:208-215.
17. Drance S, Anderson DR, Schulzer M; for the Collaborative Normal-Tension Glaucoma Study Group. Risk factors for progression of visual field abnormalities in normal-tension glaucoma. *Am J Ophthalmol*. 2001;131:699-708.
18. Phelps CD, Corbett JJ. Migraine and low-tension glaucoma. A case-control study. *Invest Ophthalmol Vis Sci*. 1985;26:1105-1108.
19. Rose KM, Wong TY, Carson AP, Couper DJ, Klein R, Sharrett AR. Migraine and retinal microvascular abnormalities: the Atherosclerosis Risk in Communities Study. *Neurology*. 2007;68:1694-1700.
20. Iafe NA, Phasukkijwatana N, Chen X, Sarraf D. Retinal capillary density and foveal avascular zone area are age-dependent: quantitative analysis using optical coherence tomography angiography. *Invest Ophthalmol Vis Sci*. 2016;57:5780-5787.
21. Akil H, Huang AS, Francis BA, Sadda SR, Chopra V. Retinal vessel density from optical coherence tomography angiography to differentiate early glaucoma, pre-perimetric glaucoma and normal eyes. *PLoS One*. 2017;12:e0170476.
22. Headache Classification Committee of the International Headache Society. The International Classification of Headache Disorders, 3rd edition (beta version). *Cephalalgia*. 2013;33:629-808.
23. Campbell JP, Zhang M, Hwang TS, et al. Detailed vascular anatomy of the human retina by projection-resolved optical coherence tomography angiography. *Sci Rep*. 2017;7:42201.
24. Schneider CA, Rasband WS, Eliceiri KW. NIH image to ImageJ: 25 years of image analysis. *Nat Methods*. 2012;9:671-675.
25. Di G, Weihong Y, Xiao Z, et al. A morphological study of the foveal avascular zone in patients with diabetes mellitus using optical coherence tomography angiography. *Graefes Arch Clin Exp Ophthalmol*. 2016;254:873-879.
26. de Carlo TE, Chin AT, Bonini Filho MA, et al. Detection of microvascular changes in eyes of patients with diabetes but not clinical diabetic retinopathy using optical coherence tomography angiography. *Retina*. 2015;35:2364-2370.
27. Minvielle W, Caillaux V, Cohen SY, et al. Macular microangiopathy in sickle cell disease using optical coherence tomography angiography. *Am J Ophthalmol*. 2016;164:137-144.e1.
28. Sanfilippo CJ, Klufas MA, Sarraf D, Tsui I. Optical coherence tomography angiography of sickle cell maculopathy. *Retin Cases Brief Rep*. 2015;9:360-362.
29. Chen X, Rahimy E, Sergott RC, et al. Spectrum of retinal vascular diseases associated with paracentral acute middle maculopathy. *Am J Ophthalmol*. 2015;160:26-34.e1.
30. McDonald WI, Sanders MD. Migraine complicated by ischaemic papillopathy. *Lancet*. 1971;2:521-523.
31. Scripsema NK, Garcia PM, Bavier RD, et al. Optical coherence tomography angiography analysis of perfused peripapillary capillaries in primary open-angle glaucoma and normal-tension glaucoma. *Invest Ophthalmol Vis Sci*. 2016;57:OCT611-OCT620.
32. Cankaya C, Tecellioglu M. Foveal thickness alterations in patients with migraine. *Med Arch*. 2016;70:123-126.
33. Martinez A, Proupim N, Sanchez M. Retinal nerve fibre layer thickness measurements using optical coherence tomography in migraine patients. *Br J Ophthalmol*. 2008;92:1069-1075.
34. Gipponi S, Scaroni N, Venturelli E, et al. Reduction in retinal nerve fiber layer thickness in migraine patients. *Neurol Sci*. 2013;34:841-845.
35. Demircan S, Atas M, Arik Yuksel S, et al. The impact of migraine on posterior ocular structures. *J Ophthalmol*. 2015;2015:868967.
36. Colak HN, Kantarci FA, Tatar MG, et al. Retinal nerve fiber layer, ganglion cell complex, and choroidal thicknesses in migraine. *Arq Bras Oftalmol*. 2016;79:78-81.
37. Ekinci M, Ceylan E, Cagatay HH, et al. Retinal nerve fibre layer, ganglion cell layer and choroid thinning in migraine with aura. *BMC Ophthalmol*. 2014;14:75.
38. Feng YF, Guo H, Huang JH, Yu JG, Yuan F. Retinal nerve fiber layer thickness changes in migraine: a meta-analysis of case-control studies. *Curr Eye Res*. 2016;41:814-822.
39. Gryglas A, Smigiel R. Migraine and stroke: what's the link? What to do? *Curr Neurol Neurosci Rep*. 2017;17:22.
40. Sacco S, Ricci S, Degan D, Carolei A. Migraine in women: the role of hormones and their impact on vascular diseases. *J Headache Pain*. 2012;13:177-189.
41. Lujan BJ, Roorda A, Knighton RW, Carroll J. Revealing Henle's fiber layer using spectral domain optical coherence tomography. *Invest Ophthalmol Vis Sci*. 2011;52:1486-1492.